# An Efficient AT-cut Quartz Crystal Resonator Design Tool for Activity Dip in Working Temperature Range

Shih-Yung Pao
TXC Corporation
Taoyuan, Taiwan/R.O.C.
sypao@txc.com.tw

Qiao-Qiao Pan, Min-Chiang Chao
TXC(Ningbo) Corporation
Ningbo, Zhejiang/China

***Abstract*—The work of an efficient design tool for engineers to enhance the frequency stability performance of AT-cut quartz crystal resonator in whole working temperature range is presented. Based on Mindlin's 2D AT-cut plate model, the design tool is a finite element analysis(FEA) program to simulate quartz plate vibration with partial electrodes(mass loading), finite dimensions(free edge), piezoelectric and temperature effects. The simulation and experiment results, including mode chart, electrical response and frequency-temperature characteristics, of a 3.2mm by 2.5mm 40MHz resonator are shown in this study. Finally, an activity-dip-contour-map which locates the high frequency-temperature stability zone is constructed and it guides engineers to do a robust design.**

## I. INTRODUCTION

As a key frequency device in almost all electric circuits, AT-cut quartz resonator should be very accurate and high stability, and therefore could not be designed by experiments or trial and error only. Mindlin[1],[2] did a series of work in crystal plate vibration as the base of AT-cut quartz resonator analysis. Lee[3] constructed a FEA program based on Mindlin's 2D model to analyze pure mechanical crystal plate vibration without piezoelectric effects. Yong and Wang[4],[5] extended the work to 3D FEA and some details, like frequency-temperature characteristics and quality factor. Today, some commercial FEA software could also simulate quartz plate vibration. However, it is time consuming to analyze quartz resonator by general commercial FEA programs because of the anisotropic structure and aspect ratio (length/width to thickness) of the quartz plate. Hence, an efficient and accurate enough design tool for modern quartz crystal resonator is always desired.

In this study, a 2D AT-cut quartz plate finite element model based on Mindlin's 2D theory is built. By the weak coupling of quartz, the pure mechanical vibration and piezoelectric effects are considered separately in the FEA to enhance the calculation efficiency. The simulation mode charts by 2D and 1D model show 2D model could contain more complete modes of quartz crystal plate. Due to including piezoelectric effects in the FEA program, the simulation electrical response (at room temperature) and frequency activity dip (in working temperature range) match the experiment results very well.

Today's high volume quartz crystal resonators' business is quite challenging. Cost reduction and maintain high quality is the key for survive. Engineers should take care wide temperature range activity dips of resonators, and this makes argues inside about design and process control. For shortening the development time and saving the cost of frequency temperature stability testing, an activity-dip-contour-map is introduced. The ordinate and abscissa of the map are the length and width of the electrode (or quartz plate), respectively. And the contour level shows the frequency activity dip (in ppm) due to working temperature change. The simulation activity-dip-contour-map is similar to the experiment results and could help engineers to choose a comfortable zone for producing.

## II. TWO-DIMENSIONAL AT-CUT QUARTZ PLATE MODEL

Considering a rectangular thin crystal plate shown in Figure 1. the width, length and thickness of the plate are 2c, 2a and 2b, respectively, and it is partially plated by metal as electrodes with 2W by 2L dimension.

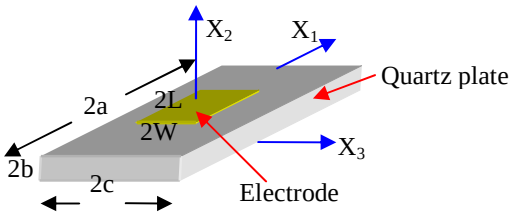


Figure 1. A rectangular crystal plate with electrodes

The equations of motion obtained from Mindlin's 2D plate theory[6]

$$\begin{cases} c_{ijkl}^{(0)}\left(u_{k,li}^{(0)}+\delta_{2l}u_{k,i}^{(1)}\right)+e_{kij}^{(0)}\varphi_{,ki}^{(0)}+T_{j}^{(0)}=\rho\ddot{u}_{j}^{(0)} \\ e_{kij}^{(0)}\left(u_{j,ki}^{(0)}+\delta_{2i}u_{j,k}^{(1)}\right)-\varepsilon_{ij}\varphi_{,ij}^{(0)}+D^{(0)}=0 \\ c_{abcd}^{(1)}u_{d,ca}^{(1)}+e_{cab}^{(1)}\varphi_{,ca}^{(1)}-3b^{-2}\left[c_{2bkl}^{(0)}\left(u_{l,k}^{(0)}+\delta_{2k}u_{l}^{(1)}\right)+e_{a2b}^{(0)}\varphi_{,a}^{(0)}+e_{22b}^{(0)}\varphi^{(1)}\right]+T_{b}^{(1)}=\rho\ddot{u}_{b}^{(1)} \\ e_{cab}^{(1)}u_{b,ca}^{(1)}-\varepsilon_{bc}\varphi_{,bc}^{(1)}-3b^{-2}\left[e_{2ijl}^{(0)}\left(u_{j,i}^{(0)}+\delta_{2i}u_{j}^{(1)}\right)-\varepsilon_{a2}\varphi_{,a}^{(0)}-\varepsilon_{22}\varphi^{(1)}\right]+D^{(1)}=0 \end{cases} \quad (1)$$

Preprint for the 2011 Joint Conference of the IEEE International Frequency Control Symposium & European Frequency and Time Forum, San Francisco, California, USA , May 1-5, 2011

where:

$u^{(0)}$, $u^{(1)}$: the zero and first order of mechanical displacement, and $i, j, k, l = 1,2,3$; $a, b = 1,3$

$\varphi^{(0)}$, $\varphi^{(1)}$: the zero and first order of electrical potential

$T^{(0)}$, $T^{(1)}$: the zero and first order of stress

$D^{(0)}$, $D^{(1)}$: the zero and first order of electrical displacement

$c, e, \varepsilon$: the components of elastics stiffness, piezoelectric stress constant and dielectric permittivity of AT-cut quartz plate, respectively

Defining zero order mechanical strain ($\nu$), mechanical stress ($P$, $Q$), electric field ($\beta$) and electric stress ($P_E$, $Q_E$); and first order mechanical strain ($\chi$), mechanical stress ($M$), electric field ($\eta$) and electric stress ($M_E$) as shown in Figure 2. and Figure 3.

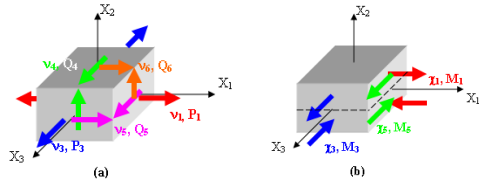


Figure 2. The sketch of strains and stresses: (a)zero order; (b) first order

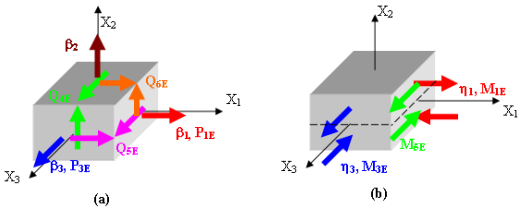


Figure 3. The sketch of electric field and stresses: (a)zero order; (b) first order

equation (2) could be express by these stress items[7]:

$$\begin{cases} P_{1,1}+Q_{5,3} & +P_{1E,1}+Q_{5E,3} & =\rho(1+R)\ddot{u}_1^{(0)} \\ Q_{4,3}+Q_{6,1} & +Q_{4E,3}+Q_{6E,1} & =\rho(1+R)\ddot{u}_2^{(0)} \\ P_{3,3}+Q_{5,1} & +P_{3E,3}+Q_{5E,1} & =\rho(1+R)\ddot{u}_3^{(0)} \\ M_{1,1}+M_{5,3}-Q_6 & +M_{1E,1}+M_{5E,3}-Q_{6E} & =\rho(1+3R)\ddot{u}_1^{(1)} \\ M_{3,3}+M_{5,1}-Q_4 & +M_{3E,3}+M_{5E,1}-Q_{4E} & =\rho(1+3R)\ddot{u}_3^{(1)} \\ D_{1,1}^{(0)}+D_{3,3}^{(0)} & -D_{d1,1}^{(0)}-D_{d3,3}^{(0)} & =-D^{(0)} \\ D_{1,1}^{(1)}+D_{3,3}^{(1)}-D_2^{(0)} & -D_{d1,1}^{(1)}-D_{d3,3}^{(1)}+D_{d2}^{(0)} & =-D^{(1)} \end{cases} \quad (2)$$

introducing a interpolation function for finite element model, and by energy densities in terms of nodal displacement and variational principle, obtained the equations of motion for one element in matrix form:

$$\begin{cases} [M^e][\ddot{U}^e]+[d_m^e][\dot{U}^e]+[K_m^e][U^e]+[K_p^e][\Psi^e]=[\hat{F}^e] \\ [K_p^e]^T[U^e]+[K_d^e][\Psi^e]=[\hat{D}^e] \end{cases} \quad (3)$$

where

$[M^e]$: element mass matrix; $[M_m^e]$: element elastic stiffness; $[d_m^e]$: element damping matrix; $[K_p^e]$: element piezoelectric coupling matrix; $[K_d^e]$: element dielectric stress matrix; $[\hat{F}^e]$ and $[\hat{D}^e]$ are the element mechanical force and surface electric displacement.

## III. Finite Element Analysis Process

Assembling all elements of FEM model to obtain the system equations in matrix form are

$$\begin{cases} [M][\ddot{U}]+[d_m][\dot{U}]+[K_m][U]+[K_p][\Psi]=[\hat{F}] \\ [K_p]^T[U]+[K_d][\Psi]=[\hat{D}] \end{cases} \quad (4)$$

Based on weak piezoelectric coupling of quartz, the elastic displacement and electrical potential are solved separately [8] to enhance the calculation efficiency. The FEA process steps are

(i) Free vibration eigenfrequency analysis

$$[M][\ddot{U}]+[K_m][U]=0 \quad (5)$$

Solve (5) as an eigenproblem to get eiengmodes $U_1$, $U_2$, … $U_n$ and the natural frequency $f_1$, $f_2$, … $f_n$.

(ii) Static electric potential due to applied voltage

$$[K_d][\Psi]=[\hat{D}'] \quad (6)$$

Give the surface-charge $[\hat{D}']$ as electric excitation signal to solve potential field $[\Psi]$ in the crystal plate.

(iii) Piezoelectric coupling stress due to potential field

$$[K_p][\Psi]=[\hat{F}'] \quad (7)$$

Substituting $[\Psi]$ form step (ii) into (7) to obtain $[\hat{F}']$, where $[\hat{F}']$ is the amplitude of piezoelectric coupling stress due to applied potential. In the next step, $[\hat{F}']$ is the external force to the pure mechanical system.

(iv) Force vibration frequency response analysis

$$[M][\ddot{U}]+[d_m][\dot{U}]+[K_m][U]=[\hat{F}']\cos\omega t \quad (8)$$

where $[\hat{F}']\cos\omega t$ is a harmonic external stress. Equation (8) is solved by mode superposition method to get the harmonic elastic displacement response

$$U = a_1U_1 + a_2U_2 + \ldots + a_nU_n$$

where $U_1$, $U_2$, … $U_n$ are the nature modes in step (i) and $a_1$, $a_2$, … $a_n$ are weights of each mode.

(v) Electric displacement and response

$$[K_p]^T[U]+[K_d][\Psi]=[\hat{D}] \quad (9)$$

Preprint for the 2011 Joint Conference of the IEEE International Frequency Control Symposium & European Frequency and Time Forum, San Francisco, California, USA , May 1-5, 2011

Substituting $U$ in step (iv) and $[\Psi]$ in step (iii) into (9) to obtain $[\hat{D}]$, the electric displacement response of the system.

(vi) Others

In the post process of the FEA, the admittance curve and equivalent circuit parameters, $C_0$, $C_1$, $R_1$ and $L_1$ .could be obtained.

## IV. Simulation and Experiment Results

A 3.2mm by 2.5mm 40MHz and 7.0mm by 5.0mm 61.44MHz resonator design examples, including mode charts, frequency response verification, temperature stability verification and activity-dip-contour-map, are presented in this section.

### A. *Mode charts by simulation*

The simulation mode charts of a 3.2mm by 2.5mm 40MHz resonator by 2D FEA model and 1D model are shown in Figure 4. and Figure 5. respectively. The former could calculate more complete modes of AT-cut quartz plate and make the simulation more accurate.

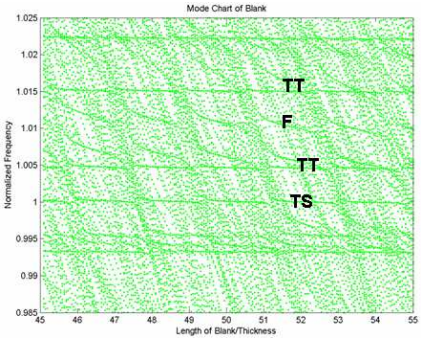


Figure 4. A 3.2mm by 2.5mm 40MHz simulation mode chart by 2D FEA model

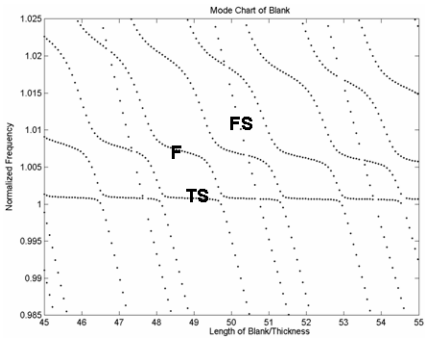


Figure 5. A 3.2mm by 2.5mm 40MHz simulation mode chart by 1D mode

### B. *Verification in freauency response*

Considering the piezoelectric effects as a force excitation in (8), the program calculates the modes “existence obviously”. The response Figure 6. shows there are three modes will be measured easily in real products as Figure 6.

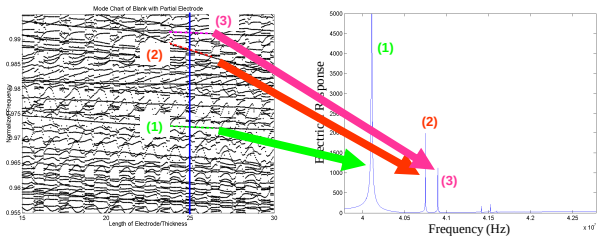


Figure 6. Simulation electrical response

We can plot the mode shape of U1(displacement in X1-axis direction) of modes (1), (2), and (3) in Figure 6. along length and width of the quartz plate, and identify mode (1) is thickness shear and mode (2) and (3) are thickness shear inharmonic overtones. The results were also check by using experiment data. In Figure 7. the left and right chats are the response by simulation and experiment, respectively. The frequency of three strong modes are marked on the simulation charts (the frequency in the parenthesis are experiment data). These two results matched very well.

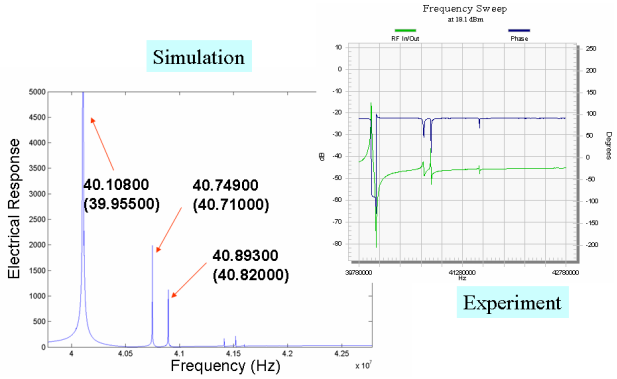


Figure 7. Verification in freauency response

### C. *Verification in frequency-temperature stability*

In Figure 8. the left and right chats are the frequency-temperature stability curves by simulation and experiment, respectively. There are activity dips around 16 $^{o}$C and 40 $^{o}$C in both calculating and testing data; that means this FEA design tool could simulate the frequency-temperature characteristics very well in the whole working temperature range.

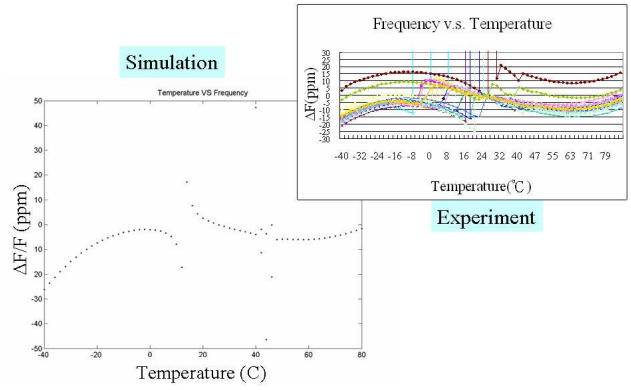


Preprint for the 2011 Joint Conference of the IEEE International Frequency Control Symposium & European Frequency and Time Forum, San Francisco, California, USA , May 1-5, 2011

Figure 8. Verification in freauency temperature stability

### D. *Activity dip contour map*

Traditionally, a crystal resonator designer should work hard to test many dimension combinations of quartz plate and electrode to verify the frequency-temperature stability performance of each size. These trial and error works make the cost of products development high; however, it spends too much time to simulate temperature characteristics by general commercial FEA program.

The design tool in this study could calculate the activity dip across the whole working temperature fast. Because of its high efficiency, it could finish the simulation for hundreds of different size in a few days with a common PC.

Figure 9 is a sketch of activity-dip-contour-map. The abscissa and ordinate are the length and width of crystal plate or electrode. The vertical axis is the activity dip of each size. The valleys on the map are "good" zones, but the peaks on the map are "bad" zones.

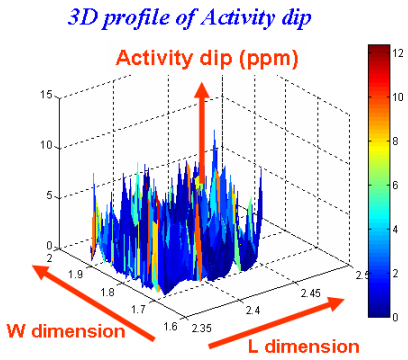


Figure 9. Activity-dip-contour-map

In Figure 10. the left and right chats are the activity-dip-contour-map by simulation and experiment, respectively. It is a 7.0mm by 5.0mm 61.44MHz design example. The main simulation conditions are:

(i) 16 steps in width, 16 steps in length

(ii) -30 $^{o}$C to 85$^{o}$C in 2$^{o}$C step

(iii) Total simulation time: 5 days by PC 2.4GHz CPU with 4GB memory

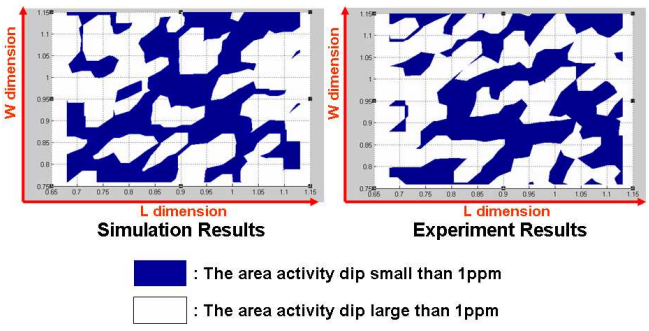


Figure 10. Simulation design map v.s. testing data

Due to some limitation of the FEA model and process variation, the activity-dip-contour-map by calculation and testing does not match very well, but it still could guide engineers to start their work in a better base for robust design.

## V. Conclusion

A 2D Mindlin plate FEA model considering mechanics, piezoelectrical, and dielectrical effects is constructed. As quartz weak coupling characteristics, the simulation efficiency could be enhanced by calculating the mechanics and electrical response separately. The simulation results of frequency response in room temperature and the activity dip characteristics in working temperature are verified. The simulation tool can provide direct-feeling about design robustness and still need to improve to consider more factors inside model. More study activities between company and academic resources are needed.

## References


[1] R.D. Mindlin, "High frequency vibrations of plated, crystal plates," *Progress* in Applied Mechanics, The Prager Anniversary Volume, Macmillan, New York, pp. 73–84, 1963.

[2] R.D. Mindlin and W.J. Spencer, "Anharmonic, thickness-twist overtones of thickness-shear and flexural vibration of rectangular, AT-cut quartz plates," *The Journal of the Acoustical Society of America*, vol. 42, no. 6, pp 1268-1277, Dec. 1967.

[3] P.C.Y. Lee, C. Zee, and C.A. Brebbia, "Thickness-shear, thickness-twist, and flexural vibration of rectangular AT-cut quartz plates with patch electrodes," in *Proc. of Freq. Control Symp.*, pp 108-119, 1978.

[4] J. Wang, Y.K. Yong, and T. Imai, "High order plate theorey based finite element analysis of the frequency-temperature relations of quartz crystal resonators," in *Proc. of Freq. Control Symp.*, pp 956-963, 1998.

[5] Y.K. Yong, W. Wei, M. Tanaka, and T. Imai, "Three dimensional finite elements and their relationships to Mindlin's higher order plate theory in quartz crystal plate," in *Proc. of Freq. Control Symp.*, pp 791-794, 2001.

[6] R.D. Mindlin, "High frequency vibration of piezoelectric crystal plates," *Int. J. Solids Structures*, vol. 8, pp 895-906, 1972.

[7] S.Y. Pao, *A theoretical and experimental study of advanced AT-cut quartz and piezoelectric thin film resonator*, thesis in the Institude of Applied Mechanics, for the Degree of Doctor of Philosophy at National Taiwan University, Taipei, Taiwan, June, 2009.

[8] S.Y. Pao, M.K. Chao, C.S. Lam, and P.Z. Chang, "An efficient numerical method in calculating the electrical impedance different modes of AT-cut quartz crystal resonator," in *Proc. of Freq. Control Symp.*, pp 396-400, 2004.



Preprint for the 2011 Joint Conference of the IEEE International Frequency Control Symposium & European Frequency and Time Forum, San Francisco, California, USA , May 1-5, 2011